analytical chemistry

Article

pubs.acs.org/ac

Nanopore-Based Selective Discrimination of MicroRNAs with Single-Nucleotide Difference Using Locked Nucleic Acid-Modified Probes

Dongmei Xi,[†] Jizhen Shang,[‡] Enguo Fan,[§] Jinmao You,[‡] Shusheng Zhang,*[,†] and Hua Wang*[,‡]

[†]Shandong Provincial Key Laboratory of Detection Technology for Tumor Makers, College of Chemistry and Chemical Engineering, Linyi University, Linyi 276005, People's Republic of China

[‡]Shandong Province Key Laboratory of Life-Organic Analysis, College of Chemistry and Chemical Engineering, Qufu Normal University, Qufu 273165, People's Republic of China

[§]Institute of Biochemistry and Molecular Biology, Zentrum für Biochemie und Molekulare Zellforschung, University of Freiburg, Freiburg D-79104, Germany

Supporting Information

ABSTRACT: The accurate discrimination of microRNAs (miRNAs) with highly similar sequences would greatly facilitate the screening and early diagnosis of diseases. In the present work, a locked nucleic acid (LNA)-modified probe was designed and used for α-hemolysin (α-HL) nanopore to selectively and specifically identify miRNAs. The hybridization of the LNA probe with the target miRNAs generated unique long-lived signals in the nanopore thus facilitated an accurate discrimination of miRNAs with similar sequences, even a single-nucleotide difference. Furthermore, the developed nanopore-based analysis with LNA probe could selectively detect target miRNAs in a natural serum background. This selective and sensitive approach may be highly valuable in the detection of clinically relevant biomarkers in complex samples.

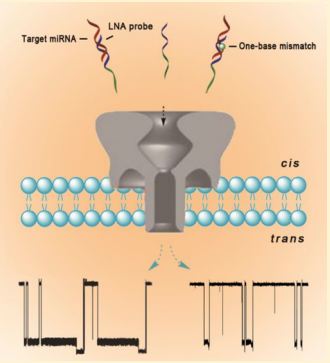

MicroRNA specifies a group of short noncoding RNA molecules that can complement to a part of one or more mRNAs, thereby resulting in such as translational inhibition or degradation of mRNA, which eventually regulates gene expression.[1,2] Besides extensive use in RNA silencing therapy, accumulated evidence suggests that the expression levels of miRNA correlate with various diseases based on the observation that different miRNA expression patterns and profiles are found in distinct types of cancer.[3,4] Therefore, the levels of miRNAs in tissues or biofluids like blood can be investigated and used as a diagnostic biomarker to screen, monitor or early diagnose of cancer.[4−8] However, because of the very small size, highly homologous sequences, and sometimes very low level expression of miRNA, accurate measurement of circulating miRNAs remains a highly challenging task. Therefore, a rapid, convenient, sensitive, and selective miRNA detection technology is highly desired.

Currently, the common miRNA detection methods include microarrays and quantitative reverse-transcription polymerase chain reaction (qRT-PCR) assays. While the microarray-based technique is amenable to assess genome-wide expression profiles of miRNAs and qPCR is convenient to quantify miRNA,[9] these methods may generally suffer from some disadvantages like the error-prone amplification, cross-hybridization, and a lack of suitable internal controls.[10,11] Other methods using a dye or radioactivity for labeling or techniques based on colorimetry, bioluminescence, enzymatic activity, and electrochemistry have also been developed or proposed,[12,13] but they are lacking sufficient selectivity and are time-consuming. Over the past two decades, the nanopore has emerged as an attractive, powerful, and sensitive single-molecule platform that has been used for a wide range of applications including rapid gene sequencing[14−17] and the detection of various analytes such as metal ions,[18,19] PEG polymer,[20,21] DNA and microRNA,[22−24] DNA−protein interactions,[25] peptides,[26,27] protein and trypsin in the mixture.[28−30] Recently, it was also shown that the sensing capabilities of solid-state nanopore can be enhanced in combination with DNA origami.[31] A hand-held wireless voltage-clamp amplifier that interfaces a sensing probe of nanopore was constructed to enable a miniaturized wireless platform that can be conveniently operated with a smartphone.[32] In particular, an aerolysin nanopore was demonstrated to first exhibit impressive advantage in the discrimination of multianalytes in the mixtures, which was attributed to its narrow diameter and the strong electrostatic interactions between the aerolysin and the oligonucleotides.[33] All these advancements indicate that the nanopore technique holds a great potential for wide practical applications. To enable an effective detection of miRNA, a sensitive nanopore sensor is critically important. While extensive efforts have been made to specifically measure

Received: July 10, 2016
Accepted: October 13, 2016
Published: October 13, 2016

DOI: 10.1021/acs.analchem.6b02620
Anal. Chem. 2016, 88, 10540−10546

miRNA,[22] it is still a big challenge to accurately discriminate between miRNAs having highly similar sequences, particularly those with only one-base mismatch, in complex biological samples.

Locked nucleic acids (LNAs) refer to nucleic acid analogues, in which the 2′ oxygen and 4′ carbon are bridged, thus, locked in the ribose moiety.[34,35] The base stacking and backbone preorganization are therefore enhanced by the locked ribose conformation that significantly increases the hybridization properties (i.e., melting temperature) of nucleotides. Such a unique property of higher base-pairing ability makes LNA an ideal tool when higher binding strength and specificity are desired like in microarray profiling,[36] qPCR,[37] and micromagnetic beads,[38] as well as in situ hybridization.[39] In the present work, we exploited this unique property of LNA to design LNA-modified probe to identify miRNAs with high specificity in α-hemolysin (α-HL) nanopore (Figure 1). The

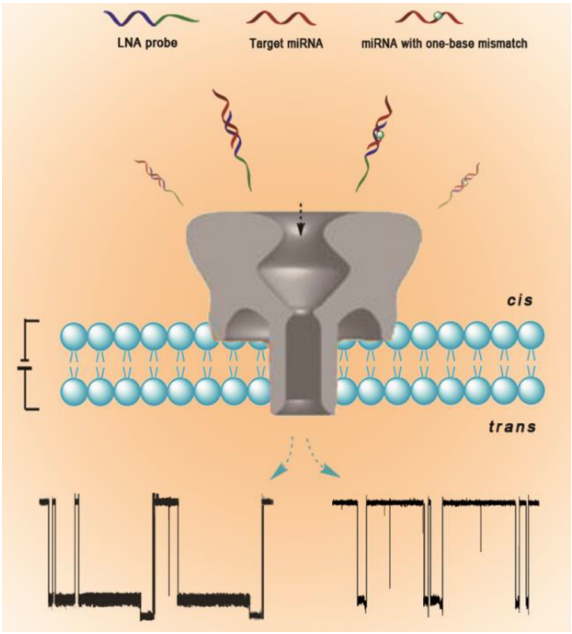

Figure 1. Illustration of LNA probe-enabled discrimination of miRNAs with single-nucleotide difference in nanopore. The probe contains a capture domain (blue) extended with a poly d$(C)_{30}$ guide (green). The capture domain used to bind the target miRNA (red) is a sequence of LNA-modified oligonucleotides. Driven by the transmembrane voltage, the LNA probe/miRNA duplex generated unique two-level and single-level long blocks that can be used to discriminate miRNAs with a single-nucleotide difference in a visual way.

LNA probe could discriminate between miRNAs with high sequence similarities, even a single-base pair mismatch. Furthermore, this nanopore-based analysis strategy facilitated the highly selective detection of target miRNAs in serum samples.

EXPERIMENTAL SECTION

Reagents and Chemials. α-HL (lyophilized powder, from *Staphylococcus aureus*), decane (anhydrous, ≥99%), and diethyl pyrocarbonate (DEPC, 99%) were purchased from Sigma-Aldrich (St. Louis, MO, U.S.A.). 1,2-Diphytanoyl-*sn*- glycero-3-phosphocholine (chloroform, ≥99%) was purchased from Avanti Polar Lipids Inc. (Alabaster, AL, U.S.A.). All of the other chemicals were of analytical grade unless otherwise indicated. All miRNAs and LNA-modified probes were synthesized in Exiqon (Denmark). The DNA probes were synthesized in Sagon (Shanghai, China). All polymers were dissolved in RNAase-free water to 100 μM as stocks. Before the nanopore measurement, the miRNAs, probe, and their mixtures at desired concentrations were heated to 90 °C for 5 min, then gradually cooled to room temperature. All solutions for analytical studies were prepared with ultrapure water (reaching a resistivity of 18.2 MΩ cm at 25 °C). The ultrapure water used in the preparation of miRNA was treated with DEPC.

Nanopore Electrical Recording. The nanopore electrical recording was conducted according to the previous studies.[40,41] The lipid bilayer membrane was formed spanning a 150 μm orifice in the center of a Delrin bilayer cup (Warner Instruments, Hamden, CT) that was partitioned into two chambers, which are termed *cis* and *trans*. Unless otherwise stated, the electrolyte solutions on each side of the bilayer contained 1.0 M KCl and were buffered with Tris - EDTA (10 mM Tris, 1 mM EDTA, pH = 7.8). The α-HL was injected adjacent to the aperture in the cis chamber, and the pore insertion was determined by a well-defined jump in the current value. Once a stable single-pore insertion was detected, the DNA or miRNA solution was added to the *cis* chamber, proximal to the aperture. The current trace was amplified and measured via an Integrating Patch Clamp (Axon Instruments, Forest City, CA) instrument with a 5 kHz lowpass Bessel filter. Data were acquired at a sampling rate of 10 kHz by using a DigiData 1440A converter and a PC running PClamp 10.6 (Axon Instruments, Forest City, CA). Analysis of data was performed using OriginLab 8.0 (OriginLab Corporation, Northampton, MA, U.S.A.). Nanopore measurements were conducted at 25 ± 2 °C.

RNA Extraction from Serum and miRNA Quantification by qRT-PCR. The let-7b was spiked into the normal human serum (10%, v/v). RNAs containing miRNAs were extracted from 40 μL of serum using the mirVana miRNA Isolation Kit (Ambion) according to the manufacturer's protocol. The final elution volume was 100 μL. The yields of RNAs were determined using a NanoDrop 2000 spectrophotometer (Thermo Scientific, U.S.A.).

qRT-PCR was used for absolute quantification of miRNAs. For preparation of standard curve, 10-fold serial dilutions of synthetic let-7b oligonucleotides were prepared to cover six points of a logarithmic range, reverse transcribed, and analyzed by qPCR. For each standard or sample, reverse transcription reaction consisted of 1 μL miRNA, 2 μL of Specific Stem-Loop RT Primer (Applied Biosystems, U.S.A.), 2 μL of PrimerScript Buffer (TaKaRa, Japan), and 0.5 μL of PrimerScript RT Enzyme Mix I (TaKaRa, Japan), in a total volume of 10 μL. Reactions were performed in a GeneAmp PCR System 9700 (Applied Biosystems, U.S.A.) for 15 min at 37 °C, followed by heat inactivation of reverse transcription for 5 s at 85 °C. The 10 μL reaction mix was then held at −20 °C.

Real-time PCR was performed using LightCycler 480 II Real-time PCR Instrument (Roche, Swiss) with 10 μL of PCR reaction mixture that included 1 μL of cDNA, 5 μL of 2 × LightCycler 480 Probes Master (Roche, Swiss), 0.5 μL of TaqMan MicroRNA Assays (Applied Biosystems, U.S.A.), and 3.5 μL of nuclease-free water. Reactions were performed in a 384-well optical plate (Roche, Swiss) by the incubation at 95 °C for 10 min, followed by 40 cycles of 95 °C for 10 s, 60 °C for 30 s. Each sample was run in triplicate for the analysis. The

DOI: 10.1021/acs.analchem.6b02620
Anal. Chem. 2016, 88, 10540−10546

concentrations of the let-7b were calculated based on the standard curve.

RESULTS AND DISCUSSION

Detection Profile of miRNAs with a LNA Probe. The let-7 tumor-suppressing miRNAs function as tumor suppressors in lung cells and their reduced expression in human lung cancers is associated with shortened postoperative survival.[42] In the present work, we used the let-7 miRNA family as the targets (Figure 2a and Supporting Information, Table S1). The

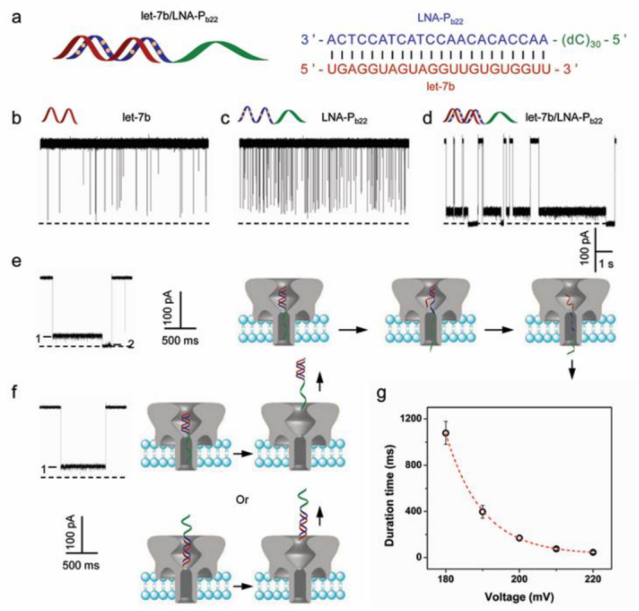

Figure 2. Detection of miRNA using LNA-P_{b22} probe. (a) Sequences of the LNA-P_{b22} probe and the target let-7b. The current traces of (b) let-7b, (c) LNA-P_{b22}, and (d) let-7b/LNA-P_{b22} hybrids, were monitored at +180 mV in solutions containing 1 M KCl buffered with 10 mM Tris (pH 7.8). The concentrations of let-7b, LNA-P_{b22}, and let-7b/LNA-P_{b22} complex were 500 nM. (e) A typical two-level long block generated by the let-7b/LNA-P_{b22} complex. Bottom: A diagram showing the molecular configurations of the hybrid dissociation and translocation. (f) Single-level block generated by a trapped let-7b/LNA-P_{b22} hybrid that exited the pore from the *cis* entrance without translocation. Either the single or duplex part of the hybrid might enter the vestibule first. (g) Duration time vs applied voltage for let-7b/LNA-P_{b22} blocks featuring two or multilevel transition for unzipping. A single-exponential function was used to fit the durations from +180 to +220 mV.

detection probe LNA-P_{b22} contains a 22 base LNA-modified sequence that was designed to specifically hybridize with the target miRNAs (Figure 2a). This probe was extended at the 5′ end with a sequence of poly(dC)$_{30}$, which acts as a guide to lead the miRNA/probe complex to enter the vestibule of the nanopore formed by α-HL, a well-studied bacterial derived toxin.[43] To test the ability of LNA-P_{b22} probe for let-7b miRNA recognition, we analyzed the events of all analytes, including the miRNA, the probe, and their hybrids, respectively. Figure 2 shows the current traces for let-7b, LNA-P_{b22}, and the hybrids added on the *cis* side of the nanopore at an applied potential of +180 mV. The addition of let-7b and LNA-P_{b22} probe produced many spike-like short blocks with durations of 0.53 ± 0.01 and 0.14 ± 0.01 ms, respectively (Figure S1). In a sharp contrast, the let-7b/LNA-P_{b22} complex generated remarkably long blocks that could last for 916.35 ± 88.76 ms (Figure 2d). More interestingly, unique two-level long blocks were identified emerging from Level 1 to Level 2 (Figure 2e), which were not observed in the presence of let-7b or LNA-P_{b22} alone. Herein, these long-lived blocks should be attributed to the formation of stable let-7b/LNA-P_{b22} hybrids that would interact with the nanopore.

To better understand the events produced by the let-7b/LNA-P_{b22} hybrids, we then selected typical blocks for a detailed analysis. Figure 2e illustrates a representative two-step current block that contains Level 1 and Level 2. Here, I_0 was defined as the current of open pore and I as the block current when analytes stayed inside the pore. Hence, the ratios of the two current levels are assigned as I_1/I_0 and I_2/I_0, respectively. The Level 1 state significantly reduced the nanopore current, with an I_1/I_0 of 0.85 ± 0.01 (Figure S2). This state was followed by a discrete current decrease to the Level 2, which fully reduced the pore current. The bottom panel in Figure 2e depicts the possible molecular configurations corresponding to the two-level blocks. The amplitude of Level 1 was consistent with a configuration in which the let-7b/LNA-P_{b22} duplex is trapped in the *cis* opening of the nanopore, with the guide poly(dC)$_{30}$ occupying the β-barrel. Driven by the transmembrane voltage, poly(dC)$_{30}$ within the β-barrel induces the dissociation of let-7b/LNA-P_{b22}. Due to a high binding strength between the LNA probe and the miRNA, the unzipping process is bound to overcome high energy barrier and thus leads to a strong interaction between the duplex and the nanopre. As a consequence, the subsequent translocation of LNA-P_{b22} through nanopore yields the Level 2 state, which featured the pore current reduced to zero. The let-7b in the nanocavity might either pass through the β-barrel to yield a spike-like short-lived block or return to the *cis* solution without translocation. The duplex unzipping process is consistent with previous studies,[44−48] despite the unique two-level blocks that featured such long durations were rarely observed in previous reports. The let-7b/LNA-P_{b22} hybrids also produced the single-level long blocks (Figure 2f), which had the same amplitude (I_1/I_0 = 0.85 ± 0.01) as those of the Level 1 of the two-level blocks. They were likely generated by the captured let-7b/LNA-P_{b22} hybrids that returned to the *cis* side without translocation, with the possibility that either the single or duplex part of the hybrids might enter the vestibule first. Since the long-lived blocks were only observed in the presence of let-7b/LNA-P_{b22} complex, they could serve as the signatures for let-7b identification.

Higher voltage can not only enhance the unzipping of the hybrids but also accelerate their translocation.[22] As expected, when the voltage increased to +200 mV, a number of multilevel long blocks were observed in the current traces of the let-7b/LNA-P_{b22} hybrids (Figure S3a). They should be contributed by the unzipping and translocation of those hybrids through the nanopore driven by the high voltage (Figure S3b). Furthermore, the voltage-dependent studies revealed that the duration time of long-lived blocks that are featuring two or multilevel transition for unzipping decreased exponentially when the applied voltage increased from +180 to +220 mV (Figures 2g and S4), which thus confirms the translocation of let-7b/LNA-P_{b22} through the nanopore.

LNA Enables Discrimination of Single Nucleotide Mismatch. It was shown that miRNAs with a single-nucleotide difference can be statistically discriminated using an oligonucleotide probe, by which the obtained block duration time was

DOI: 10.1021/acs.analchem.6b02620
Anal. Chem. 2016, 88, 10540−10546

about 3−4-fold for perfectly matched over one-mismatched miRNA/probe hybrids.[22] However, theoretical calculation suggested that there should be at least 8−10-fold duration difference in order to achieve 90% discrimination accuracy.[22,49] Therefore, we next sought to examine if LNA-probes can improve discrimination accuracy. To this end, we selected the let-7 family members let-7a and let-7c, which have two or one nucleotide differences compared with let-7b, respectively, to perform the test. Figure 3a shows the current traces for the

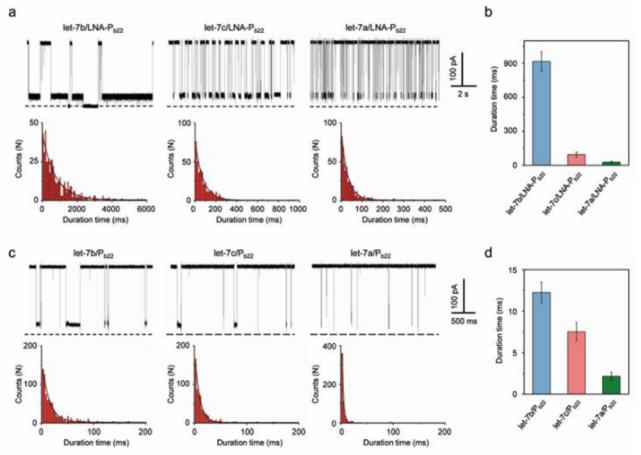

Figure 3. Discrimination of miRNAs that contain one or two-base mismatched nucleotides. (a) Probe LNA-P_{b22} was used to detect let-7a, let-7b, and let-7c. The current across the nanopore was monitored at +180 mV in 1 M KCl. Upper: current traces. Lower: the histograms of duration times that were each fitted by the exponential function. (b) Comparison of the duration times of the three hybrids at +180 mV using LNA-P_{b22} probe. (c) Detection of let-7a, let-7b, and let-7c using the DNA probe P_{b22} at +180 mV. (d) Comparison of the duration of the three hybrids using P_{b22} probe.

hybrids let-7b/LNA-P_{b22}, let-7c/LNA-P_{b22}, and let-7a/LNA-P_{b22} monitored at +180 mV. While the fully hybridized let-7b/LNA-P_{b22} generated numerous two-level or single-level long blocks with a duration of 916.35 ± 88.76 ms (Figure 3a,b), the two-level long blocks were rarely observed for the single-base mismatched let-7c/LNA-P_{b22} hybrids. Instead, a small number of multilevel blocks and numerous single-level blocks were identified with a duration of 95.62 ± 21.46 ms, which is about 10 times shorter than those obtained by let-7b/LNA-P_{b22}. In case of two-base mismatched let-7a/LNA-P_{b22} hybrids, more multilevel blocks with a duration of 28.31 ± 8.15 ms, which are about 32 times shorter compared with let-7b/LNA-P_{b22} blocks, were observed. These results suggest that, at the potential of +180 mV, the perfectly matched let-7b/LNA-P_{b22} is highly stable against dehybridization, while a one- or two-base mismatch introduced in the miRNA/LNA-probe duplex greatly destabilizes its hybridization. As a result, the current traces for let-7a, let-7b, and let-7c can be easily discriminated visually. When the potential was lowered to +100 mV; however, all of the three hybrids produced "permanent" current blocks that require the application of a negative potential to unblock the pore (Figure S5) and, thus, could not be differentiated. This is understandable given that the binding of LNA-P_{b22} to any of the three miRNAs (let-7a, let-7b, and let-7c) was so stable that the low potential of +100 mV could not unzip any of the duplexes.

The high discrimination efficiency of LNA-P_{b22} is believed to result from the incorporation of LNA in the probe because when a 22 nt DNA probe without LNA modification was used (Figure 3c,d), the differences of the block duration between perfectly matched miRNA/probe (12.23 ± 1.27 ms) and one or two mismatches are only 1.6 and 5.7 times as similar as previously reported.[22] Based on the block durations, a miRNA/LNA complex shows much higher hybridization strength compared with the same sequence of a miRNA/DNA complex. This improved hybridization strength thus leads to greater specificity in binding to complementary miRNAs. All together, the combination of the LNA with the nanopore technology possesses a sufficient high specificity in resolving the miRNA family members with even a single-nucleotide difference.

Enhancing the Mismatch Discrimination with a Shorter Probe. Given that the length of the probe is closely related to the stability of its hybridization with the target, the effects of probe length on the mismatch discrimination capability were investigated. When the LNA probe was shortened from 22 to 15 nt (Figure 4a), the fully hybridized

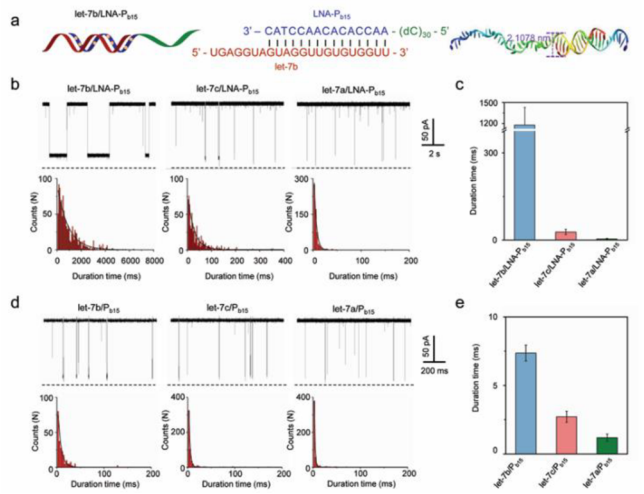

Figure 4. Discrimination of let-7 miRNAs with one- or two-base mismatch using shorter probes. (a) Sequences of the probe LNA-P_{b15} and the structure of the let-7b/LNA-P_{b15} complex in 1 M KCl at pH 7.8, with the molecular dynamic simulation detailed in Supporting Information. (b) Upper: current traces recorded at +100 mV in 1 M KCl. Lower: histograms of duration time, each of which was fitted by the exponential function. (c) Comparison of the duration times of three hybrids at +100 mV using LNA-P_{b15} probe. (d) Detection of let-7a, let-7b, and let-7c using the DNA probe P_{b15} at +180 mV. (e) Comparison of the durations of the three hybrids using P_{b15} probe.

let-7b/LNA-P_{b15} produced a large number of single-level long blocks that lasted for a long period of 1.18 ± 0.25 s at a low voltage of +100 mV, which is among the most commonly used moderate voltages (Figure 4b). The single-level block was still likely formed by the trapped duplex that was released back to the *cis* solution without translocation. This is consistent with the structural analysis of let-7b/LNA-P_{b15} complex, which suggests that the let-7b/LNA-P_{b15} hybrid (2.1078 nm wide, Figure 4a, right) can enter the vestibule from the *cis* side but cannot enter the narrowest constriction of α-HL nanopore. When we used the single mismatched let-7c/LNA-P_{b15} and two-base mismatched let-7a/LNA-P_{b15} hybrids to perform the test, the obtained blocks had durations of 27.91 ± 9.32 ms and 4.57 ± 1.55 ms (Figure 4b,c), which are about 42 and 260 times

DOI: 10.1021/acs.analchem.6b02620
Anal. Chem. 2016, 88, 10540−10546

shorter compared with those of let-7b/LNA-P_{b15}, respectively. This higher discrimination factor enables an easier differentiation of the current traces for let-7a, let-7b, and let-7c visually, indicating that the LNA-P_{b15} probe has a better mismatch differentiation for let-7b detection. As a further confirmation, a 15 nt DNA probe without LNA modification was used to discriminate let-7b from let-7a and let-7c (Figure 4d,e). The discrimination factors between a perfect match and one and two-mismatches are only 2.7 and 6.2, respectively, further demonstrating that the excellent single-base discrimination capability of the LNA-P_{b15} probe is because of the presence of LNA.

When the voltage increased from +100 to +180 mV, on the one hand, a large number of multilevel events were produced by let-7b/LNA-P_{b15} hybrids, suggesting that shortening the LNA probe increases the translocation probability of the complex. On the other, the duration of let-7b/LNA-P_{b15} blocks (73.46 ± 15.27 ms) was still up to about 12 and 50 times longer than that for let-7c/LNA-P_{b15} and let-7a/LNA-P_{b15}, respectively (Figure S6). This result, combined with the data obtained at +100 mV, indicates that enhanced discrimination ability was achieved by using the shorter probe LNA-P_{b15}, regardless of the value of the voltage applied. Herein, the hybridized complex stability seems to be a key factor in determining the mismatch discrimination and is greatly dependent on the LNA length. As for the LNA-P_{b22} probe, too much LNA is incorporated and the hybridization of the probe with either perfect match or mismatch is so stable that the hybrids would only be unzipped at very high potential; as a result, the LNA-P_{b22} probe exhibits lower selectivity. In contrast, the LNA-P_{b15} probe seems to gain an optimal LNA length thus confers a certain degree of flexibility to lower the complex stability to an optimal range, which enables the production of sufficient characteristic blocks and excellent single-nucleotide discrimination capability in a wide range of voltages.

Quantification of miRNAs. Quantitative detection of miRNAs was performed using the LNA-P_{b15} probe. As shown in Figure 5, we could verify that the frequency of let-7b/LNA-P_{b15} signature events was proportional to the let-7b concentrations ranging from 5 to 500 nM at +100 mV and the data can be fitted to a straight line in the log−log scale. The relationship can be described as the function $\log f = -1.242 + 0.749 \log[\text{let-7b}]$ ($R = 0.995$), where f is the frequency of signature events. It should be mentioned that though the α-HL pore could behave a slightly gating property, the gating events feature intensive occurrence that can be easily distinguished from the let-7b/LNA-P_{b15} signatures. Because they were not observed in the background current trace of the α-HL (Figure S7) during the tests, they could be excluded from the events used for miRNA quantification, even at low concentrations. In addition, it was reported that a gradient of salt concentration across a nanopore greatly increases the capture rate of dsDNA[50] and miRNA.[22] As expected, herein, the use of asymmetrical KCl solutions (0.5 M/3 M, *cis*/*trans*) greatly improved the detection sensitivity, thus, allowing for the measurement of the frequency of let-7b/LNA-P_{b15} events at lower concentrations ranging from 50 pM to 1 nM (Figure S8).

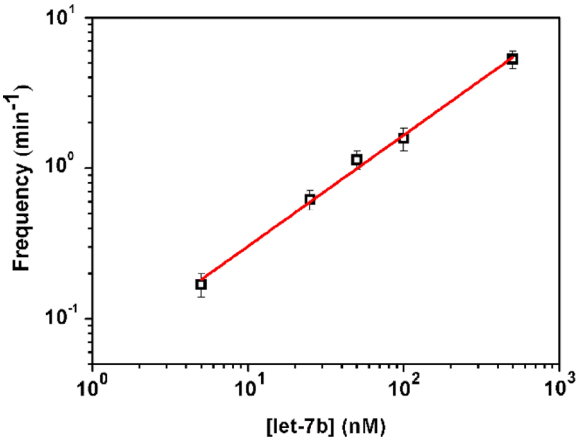

Figure 5. Quantification of miRNA let-7b using the LNA-P_{b15} probe. The concentration-dependent frequency of let-7b/LNA-P_{b15} signature events was shown. The target concentration ranges between 5 and 500 nM. Data were measured at +100 mV in 1 M KCl.

Detection of miRNA Levels in Human Serum Samples. To evaluate the applicability of the proposed nanopore analysis strategy for miRNA probing in real biological samples, let-7b was spiked into the normal human serum (10%, v/v) to be determined. While the current trace of serum samples retained a low level of noise-like spikes (Figure 6a), the addition of

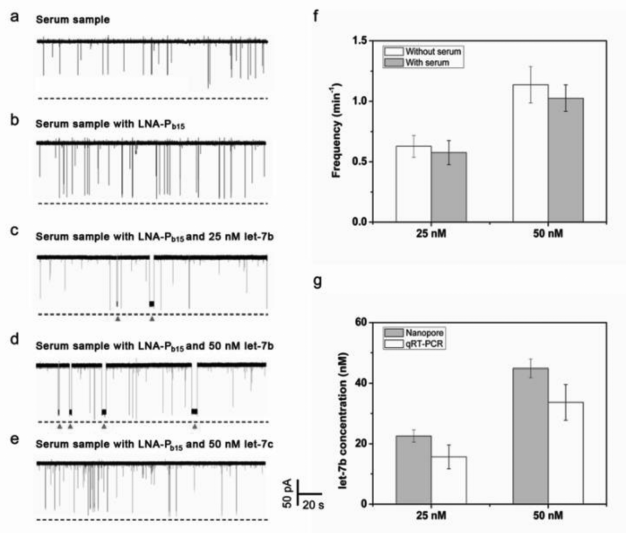

Figure 6. Detection of let-7b in human serum samples using the LNA-P_{b15} probe. Current traces for human serum in the absence (a, b, e) and presence (c, d) of target let-7b were shown. The LNA-P_{b15} probes in (b)−(e) are in concentrations of 50, 50, 100, and 100 nM, respectively. Red triangles are signature events. The current traces were recorded at +100 mV in 1 M KCl for 3 min. (f) Comparison of let-7b detection capability with and without human serum. (g) Comparison of let-7b levels measured with the nanopore and qRT-PCR method.

LNA-P_{b15} produced spike-like short blocks (Figure 6b). In a sharp contrast, the serum samples containing both let-7b and LNA-P_{b15} probe showed distinct long blocks (Figure 6c,d), whose frequencies were comparable to the samples without serum (Figure 6f). In particular, the addition of let-7c into the sample mixture produced very short events (Figure 6e), which could be easily discriminated from that of let-7b. In order to test the accuracy of the presented assay, the let-7b spiked into human serum with the same concentration was also quantified comparably using the qRT-PCR method (Figure 6g). It was found that the let-7b concentrations measured by qRT-PCR were basically in consistent to those obtained using nanopore

DOI: 10.1021/acs.analchem.6b02620
Anal. Chem. 2016, 88, 10540−10546

sensor. Therefore, the developed nanopore-based bioassay with LNA-probe has a great potential in practical applications to detect biomarkers in complex biological samples.

CONCLUSION

In the present work, a LNA-modified oligonucleotide probe has been designed to enable a selective and sensitive detection of miRNAs in the nanopore. LNA constitutes a key component of the probe and its high binding affinity to the target miRNA generates unique long-lived signals. This enables an excellent discrimination of miRNAs with single/two nucleotide difference. Compared to previous reports regarding the nanopore analysis of miRNAs, this approach could achieve a greatly enhanced mismatch discrimination by coupling nanopore technology and LNA probes. In particular, the proposed strategy exhibits an outstanding anti-interference capability and can be used to detect the target miRNAs with a high selectivity in complex biological samples, in which usually a sample preseparation is required. Therefore, such a simple, convenient, selective, and sensitive analysis approach holds a great potential for the detection applications of clinically relevant biomarkers in the early diagnosis of diseases and biomedical research fields.

ASSOCIATED CONTENT

Supporting Information

The Supporting Information is available free of charge on the ACS Publications website at DOI: 10.1021/acs.analchem.6b02620.

Sequences of miRNAs and probes used in this study (Table S1), Detection of miRNA with a LNA-modified probe (Figure S1); Histograms of blockage currents for Level 1, which was fitted by a Gauss function (Figure S2); Detection of let-7b using LNA-P_{b22} probe at +200 mV (Figure S3); Duration histograms of let-7b/LNA-P_{b22} hybrids at different voltages (Figure S4); Current traces of three complexes recorded in 1 M KCl at +100 mV (Figure S5); Duration histograms of three hybrids at +180 mV (Figure S6); The background current traces of the α-HL pore recorded in 1 M KCl at +100 mV (Figure S7); and Quantification of miRNA let-7b using the LNA-P_{b15} probe (Figure S8; PDF).

AUTHOR INFORMATION

Corresponding Authors

*E-mail: shushzhang@126.com.

*E-mail: huawangqfnu@126.com.

Notes

The authors declare no competing financial interest.

ACKNOWLEDGMENTS

This work was supported by the National Natural Science Foundation of China (21405073, 21535002), the "Innovation Team Development Plan" of the Ministry of Education Rolling Support (IRT_15R31), and the Open Funds of the State Key Laboratory of Electroanalytical Chemistry (SKLEAC201502).

REFERENCES

(1) Selbach, M.; Schwanhausser, B.; Thierfelder, N.; Fang, Z.; Khanin, R.; Rajewsky, N. *Nature* **2008**, *455*, 58−63.

(2) Bartel, D. P. *Cell* **2009**, *136*, 215−233.

(3) Garzon, R.; Calin, G. A.; Croce, C. M. *Annu. Rev. Med.* **2009**, *60*, 167−179.

(4) Ortholan, C.; Puissegur, M. P.; Ilie, M.; Barbry, P.; Mari, B.; Hofman, P. *Curr. Med. Chem.* **2009**, *16*, 1047−1061.

(5) Chen, X.; Ba, Y.; Ma, L.; Cai, X.; Yin, Y.; Wang, K.; Guo, J.; Zhang, Y.; Chen, J.; Guo, X.; Li, Q.; Li, X.; Wang, W.; Zhang, Y.; Wang, J.; Jiang, X.; Xiang, Y.; Xu, C.; Zheng, P.; Zhang, J.; Li, R.; Zhang, H.; Shang, X.; Gong, T.; Ning, G.; Wang, J.; Zen, K.; Zhang, J.; Zhang, C. Y. *Cell Res.* **2008**, *18*, 997−1006.

(6) Kosaka, N.; Iguchi, H.; Yoshioka, Y.; Takeshita, F.; Matsuki, Y.; Ochiya, T. J. *J. Biol. Chem.* **2010**, *285*, 17442−17452.

(7) Boeri, M.; Verri, C.; Conte, D.; Roz, L.; Modena, P.; Facchinetti, F.; Calabro, E.; Croce, C. M.; Pastorino, U.; Sozzi, G. *Proc. Natl. Acad. Sci. U. S. A.* **2011**, *108*, 3713−3718.

(8) Hu, Z.; Chen, X.; Zhao, Y.; Tian, T.; Jin, G.; Shu, Y.; Chen, Y.; Xu, L.; Zen, K.; Zhang, C.; Shen, H. *J. Clin. Oncol.* **2010**, *28*, 1721−1726.

(9) Wang, W. T.; Chen, Y. Q. *J. Hematol. Oncol.* **2014**, *7*, 86.

(10) Chen, C.; Ridzon, D. A.; Broomer, A. J.; Zhou, Z.; Lee, D. H.; Nguyen, J. T.; Barbisin, M.; Xu, N. L.; Mahuvakar, V. R.; Andersen, M. R.; Lao, K. Q.; Livak, K. J.; Guegler, K. J. *Nucleic Acids Res.* **2005**, *33*, e179.

(11) Li, W.; Ruan, K. *Anal. Bioanal. Chem.* **2009**, *394*, 1117−1124.

(12) Hunt, E. A.; Goulding, A. M.; Deo, S. K. *Anal. Biochem.* **2009**, *387*, 1−12.

(13) Yendamuri, S.; Kratzke, R. *Transl. Res.* **2011**, *157*, 209−215.

(14) Deamer, D.; Akeson, M.; Branton, D. *Nat. Biotechnol.* **2016**, *34*, 518−524.

(15) Branton, D.; Deamer, D. W.; Marziali, A.; Bayley, H.; Benner, S. A.; Butler, T.; Di Ventra, M.; Garaj, S.; Hibbs, A.; Huang, X.; Jovanovich, S. B.; Krstic, P. S.; Lindsay, S.; Ling, X. S.; Mastrangelo, C. H.; Meller, A.; Oliver, J. S.; Pershin, Y. V.; Ramsey, J. M.; Riehn, R.; Soni, G. V.; Tabard-Cossa, V.; Wanunu, M.; Wiggin, M.; Schloss, J. A. *Nat. Biotechnol.* **2008**, *26*, 1146−1153.

(16) Cherf, G. M.; Lieberman, K. R.; Rashid, H.; Lam, C. E.; Karplus, K.; Akeson, M. *Nat. Biotechnol.* **2012**, *30*, 344−348.

(17) Manrao, E. A.; Derrington, I. M.; Laszlo, A. H.; Langford, K. W.; Hopper, M. K.; Gillgren, N.; Pavlenok, M.; Niederweis, M.; Gundlach, J. H. *Nat. Biotechnol.* **2012**, *30*, 349−353.

(18) Braha, O.; Gu, L. Q.; Zhou, L.; Lu, X.; Cheley, S.; Bayley, H. *Nat. Biotechnol.* **2000**, *18*, 1005−1007.

(19) Wen, S.; Zeng, T.; Liu, L.; Zhao, K.; Zhao, Y.; Liu, X.; Wu, H. C. *J. Am. Chem. Soc.* **2011**, *133*, 18312−18317.

(20) Cao, C.; Ying, Y. L.; Gu, Z.; Long, Y. T. *Anal. Chem.* **2014**, *86*, 11946−11950.

(21) Movileanu, L.; Cheley, S.; Bayley, H. *Biophys. J.* **2003**, *85*, 897−910.

(22) Wang, Y.; Zheng, D.; Tan, Q.; Wang, M. X.; Gu, L. Q. *Nat. Nanotechnol.* **2011**, *6*, 668−674.

(23) Liu, N.; Jiang, Y.; Zhou, Y.; Xia, F.; Guo, W.; Jiang, L. *Angew. Chem., Int. Ed.* **2013**, *52*, 2007−2011.

(24) Wanunu, M.; Dadosh, T.; Ray, V.; Jin, J.; McReynolds, L.; Drndic, M. *Nat. Nanotechnol.* **2010**, *5*, 807−814.

(25) Tabard-Cossa, V.; Wiggin, M.; Trivedi, D.; Jetha, N. N.; Dwyer, J. R.; Marziali, A. *ACS Nano* **2009**, *3*, 3009−3014.

(26) Stefureac, I. R.; Kachayev, A.; Lee, S. J. *Chem. Commun.* **2012**, *48*, 1928−1930.

(27) Wang, H. Y.; Gu, Z.; Cao, C.; Wang, J.; Long, Y. T. *Anal. Chem.* **2013**, *85*, 8254−8261.

(28) Bell, N. A.; Keyser, U. F. *J. Am. Chem. Soc.* **2015**, *137*, 2035−2041.

(29) Kong, J.; Bell, N. A.; Keyser, U. F. *Nano Lett.* **2016**, *16*, 3557−3562.

(30) Zhou, S.; Wang, L.; Chen, X.; Guan, X. *ACS Sens.* **2016**, *1*, 607−613.

(31) Keyser, U. F. *Nat. Nanotechnol.* **2016**, *11*, 106−108.

(32) Ozel, R. E.; Kahnemouyi, S.; Fan, H.; Mak, W. H.; Lohith, A.; Seger, A.; Teodorescu, M.; Pourmand, N. *ACS Sens.* **2016**, *1*, 265−271.

(33) Cao, C.; Ying, Y. L.; Hu, Z. L.; Liao, D. F.; Tian, H.; Long, Y. T. *Nat. Nanotechnol.* **2016**, *11*, 713−718.

DOI: 10.1021/acs.analchem.6b02620
Anal. Chem. 2016, 88, 10540−10546

(34) Wahlestedt, C.; Salmi, P.; Good, L.; Kela, J.; Johnsson, T.; Hokfelt, T.; Broberger, C.; Porreca, F.; Lai, J.; Ren, K.; Ossipov, M.; Koshkin, A.; Jakobsen, N.; Skouv, J.; Oerum, H.; Jacobsen, M. H.; Wengel, J. *Proc. Natl. Acad. Sci. U. S. A.* **2000**, *97*, 5633−5638.
(35) Petersen, M.; Bondensgaard, K.; Wengel, J.; Jacobsen, J. P. *J. Am. Chem. Soc.* **2002**, *124*, 5974−5982.
(36) Tolstrup, N.; Nielsen, P. S.; Kolberg, J. G.; Frankel, A. M.; Vissing, H.; Kauppinen, S. *Nucleic Acids Res.* **2003**, *31*, 3758−3762.
(37) Denys, B.; El Housni, H.; Nollet, F.; Verhasselt, B.; Philippe, J. *J. Mol. Diagn.* **2010**, *12*, 512−519.
(38) Laschi, S.; Palchetti, I.; Marrazza, G.; Mascini, M. *Bioelectrochemistry* **2009**, *76*, 214−220.
(39) Kloosterman, W. P.; Wienholds, E.; de Bruijn, E.; Kauppinen, S.; Plasterk, R. H. *Nat. Methods* **2006**, *3*, 27−29.
(40) Rotem, D.; Jayasinghe, L.; Salichou, M.; Bayley, H. *J. Am. Chem. Soc.* **2012**, *134*, 2781−2787.
(41) Ying, Y. L.; Zhang, J.; Meng, F. N.; Cao, C.; Yao, X.; Willner, I.; Tian, H.; Long, Y. T. *Sci. Rep.* **2013**, *3*, 1662.
(42) Landi, M. T.; Zhao, Y.; Rotunno, M.; Koshiol, J.; Liu, H.; Bergen, A. W.; Rubagotti, M.; Goldstein, A. M.; Linnoila, I.; Marincola, F. M.; Tucker, M. A.; Bertazzi, P. A.; Pesatori, A. C.; Caporaso, N. E.; McShane, L. M.; Wang, E. *Clin. Cancer Res.* **2010**, *16*, 430−441.
(43) Ying, Y. L.; Zhang, J.; Gao, R.; Long, Y. T. *Angew. Chem., Int. Ed.* **2013**, *52*, 13154−13161.
(44) Jin, Q.; Fleming, A. M.; Burrows, C. J.; White, H. S. *J. Am. Chem. Soc.* **2012**, *134*, 11006−11011.
(45) Ying, Y. L.; Wang, H. Y.; Sutherland, T. C.; Long, Y. T. *Small* **2011**, *7*, 87−94.
(46) Deamer, D. W.; Branton, D. *Acc. Chem. Res.* **2002**, *35*, 817−825.
(47) Singer, A.; Wanunu, M.; Morrison, W.; Kuhn, H.; Frank-Kamenetskii, M.; Meller, A. *Nano Lett.* **2010**, *10*, 738−742.
(48) Wen, S.; Zeng, T.; Liu, L.; Zhao, K.; Zhao, Y.; Liu, X.; Wu, H. C. *J. Am. Chem. Soc.* **2011**, *133*, 18312−18317.
(49) Tian, K.; He, Z.; Wang, Y.; Chen, S. J.; Gu, L. Q. *ACS Nano* **2013**, *7*, 3962−3969.
(50) Wanunu, M.; Morrison, W.; Rabin, Y.; Grosberg, A. Y.; Meller, A. *Nat. Nanotechnol.* **2010**, *5*, 160−165.

DOI: 10.1021/acs.analchem.6b02620
Anal. Chem. 2016, 88, 10540−10546